Systematic design of ADRC-based unmanned tracked vehicle trajectory tracking with FPGA-in-the-loop validation

Momir R. Stanković[a], *Rafal* Madonski[b], *Stojadin* M. Manojlović[c]

[a] University of Defence in Belgrade, Military Academy, Belgrade, Republic of Serbia, e-mail: momir_stankovic@yahoo.com, **corresponding author**, ORCID iD: https://orcid.org/0000-0001-8371-9341

[b] Silesian University of Technology, Faculty of Automatic Control, Electronics and Computer Science, Gliwice, Republic of Poland, e-mail: madonski@polsl.pl, ORCID iD: https://orcid.org/0000-0002-1798-0717

[c] University of Defence in Belgrade, Military Academy, Belgrade, Republic of Serbia, e-mail: stojadin.manojlovic@va.mod.gov.rs, ORCID iD: https://orcid.org/0000-0003-1268-5310

https://doi.org/10.5937/vojtehg72-49983

FIELD: automatic control, control engineering, mobile robotics
ARTICLE TYPE: original scientific paper

Abstract:

Introduction/purpose: The trajectory tracking control problem in an unmanned tracked vehicle (UTV) represents a challenging task, due to unknown and unmeasurable slippage dynamics which inevitably exists during movement. Therefore, the application of standard industrial control schemes is often limited.

Methods: In this paper, an active disturbance rejection control (ADRC) scheme is proposed for the longitudinal (vehicle longitudinal velocity control) and lateral (vehicle course angle control) control channels of the UTV to collectively handle all the plant modeling uncertainties and acting slippage disturbances.

Results: A step-by-step procedure for applying the ADRC algorithm for the specific case of UTV trajectory tracking is presented. It includes systematic design, discretization as well as performance analysis and validation utilizing FPGA-in-the-loop (FIL) simulations.

ACKNOWLEDGMENT: The authors are grateful for the financial support from the University of Defence in Belgrade, Republic of Serbia, project code: VA-TT/1/21-23.

Conclusions: The proposed FIL-based validation method reduces the gap between pure simulation design (which may be too idealized) and implementation on the real vehicle (which may be time-consuming). The obtained experimental results show the advantages of the proposed control structure over standard industrial PI/PID controllers in different working conditions.

Key words: unmanned tracked vehicles, trajectory tracking, active disturbance rejection control, velocity control, PID controller, FPGA-in-the-loop, hardware validation.

Introduction

In recent years, unmanned tracked vehicles (UTVs) have received considerable attention in both civilian and military applications, mostly due to their high mobility and performance in different terrain (Nonami et al., 2013).

The control algorithms for UTVs often take into account the dynamic behavior and construction limits of the vehicle to ensure high movement performance along with sufficient robustness against external disturbances. UTVs are commonly designed without a steering mechanism and the direction of motion is changed by adjusting the angular velocities of the right and left track drive wheels. This provides a fast vehicle response to control signals with a minimum turning radius. However, complex dynamics of the interaction between the tracks and ground causes significant slippage during maneuvering (Janarthanan et al., 2012), leading to the UTV's motion being largely dependent on the terrain properties (Wong, 2022). The UTV slip models based on the tracks instantaneous centers of rotation were analyzed, for example, in (Pentzer et al., 2014) and (Lu et al., 2016), where it was shown that, besides the terrain characteristics, the important factors which significantly affect slippage dynamics are path curvature and the absolute value of the UTV lateral acceleration.

The most common tasks for unmanned vehicles are point-to-point motion, path following, and trajectory tracking (De Luca et al., 1998). The first is a stabilization problem, where the vehicle, starting from a given initial point, has to reach the desired point in space, regardless of the motion profile. Path following and trajectory tracking require motion along the defined geometric path/trajectory, where the trajectory is additionally constrained by time.

To ensure the realization of appropriate motion tasks for UTVs, different control strategies can be used. The usual choice is the time-tested PI/PID

controllers. In (Hu et al., 2019), for example, a torque-speed control strategy was proposed based on low-complexity PID controllers. The authors of (Zou et al., 2018) suggested relying on precise vehicle kinematics and dynamics models and applying control structures with back-stepping PID. Finally, in (Huang et al., 2018b), look-ahead lateral errors were used to design a PI-based path-tracking control system. The main advantages of using the PID-family controllers are their simple design, intuitive procedures for parameter settings, and straightforward implementation. However, their applications to UTVs are often limited in practice by the level of modeling uncertainties and the influence of large, unmodeled slippage dynamics. Therefore, the solutions to the problems of UTV path following and trajectory tracking on uneven terrains often have to rely in real life on using more sophisticated control techniques.

Analyzing the literature on advanced control for UTVs, one can notice three main types of governing algorithms, namely intelligent control, so-called modern control, and observer-based control, with some notable, representative works recalled below.

- The first type is usually based on fuzzy logic and neural networks (Li et al., 2020; Dai et al., 2018) or their combination with classical controllers, like those seen in (Huang et al., 2018a; Al-Jarrah et al., 2019). Although these advanced control structures can provide high trajectory tracking performance even in challenging terrains, their hardware implementation is often limited due to algorithmic complexity and resultant increased computational requirements.
- The so-called modern control approaches are mostly based on model predictive control (Mitsuhashi et al., 2019; Tao et al., 2021; Burke, 2012), adaptive control (Tang et al., 2021; Gonzalez et al., 2010; Hiramatsu et al., 2019), nonlinear control (Hong et al., 2009), or sliding mode control (Sabiha et al., 2022). Those methods, even though effective, rely either on precise modeling of UTV motion and slippage disturbance (Hong et al., 2009; Mitsuhashi et al., 2019) or utilizing a dedicated, separate function block for model parameters identification and/or slippage dynamics estimation.
- The third type of advanced control scheme for UTVs is observed-based control. In this category, an example extended Kalman filter was applied in (Tao et al., 2021) to estimate the coefficients of road resistance, thus strengthening the model predictive control's adapt-

ability to uncertain road conditions. Another example can be (Burke, 2012), where the compensation of slip disturbance was addressed using an adaptive least squares slippage estimator. In (Hiramatsu et al., 2019), a structure composed of an adaptive controller and disturbance observer was proposed for UTV angular and linear velocity estimation, where the observer was responsible for estimating the effects of slippage which in return improved the tracking performance without making the model unbearably complex.

Having analyzed the literature on UTV control, it seems that the current method landscape is missing an approach that would be a compromise between effectiveness, overall complexity as well as knowledge about the controlled system and the environment affecting it. Therefore, in this work, we propose the use of an active disturbance rejection control (ADRC) scheme (Gao, 2006), which is a general methodology known to provide robust performance, straightforward tuning and implementation, and operation not being overly dependent on the plant's mathematical model. The ADRC's recent successful industrial applications (discussed in the overview paper (Zhang et al., 2021)) are the main motivation for using it in this work for the UTV trajectory tracking control system. In fact, this is not the first time ADRC has been considered for UTVs. In (Chen et al., 2019), the authors have introduced back-stepping ADRC as their lateral control for the path-following problem, which featured an extended state observer (ESO) for jointly estimating internal model uncertainties and slippage disturbances.

The contribution of our work is the extensions provided to (Chen et al., 2019). Firstly, our research deals with the UTV trajectory tracking task, where the trajectory is additionally constrained with time. Secondly, this paper extends the scope to designing both controllers: lateral and longitudinal. Finally, in contrast to (Chen et al., 2019), we go beyond just a simulation study and perform FPGA-in-the-loop (FIL) verification. Such a methodology reduces the gap between a pure simulation design (which may be too idealized) and implementation on the real vehicle (which may be resource-consuming). With this paper, we want to show a comprehensive application of ADRC to UTVs (with all its unique characteristics and intricacies), including systematic design, performance analysis, and validation.

The paper is organized as follows. The UTV model is briefly recalled in the UTV motion model section. Then, the design of lateral and longitudinal controllers is shown in the Lateral controller design and Longitudinal controller design sections. The verification of the proposed control system is described in the Control system verification. The section entitled Conclusion summarizes the work.

UTV motion model

The kinematic model of the considered UTV can be described as:

$$\begin{pmatrix} \dot{x}(t) \\ \dot{y}(t) \\ \dot{\theta}(t) \end{pmatrix} = \begin{pmatrix} \cos\theta(t) & 0 \\ \sin\theta(t) & 0 \\ 0 & 1 \end{pmatrix} \cdot \begin{pmatrix} v(t) + v_{\mathrm{d}}(t) \\ \omega(t) + \omega_{\mathrm{d}}(t) \end{pmatrix}, \tag{1}$$

where $x(t)$ and $y(t)$ denote vehicle coordinates in the inertial coordinate system, $\theta(t)$ is the course angle of UTV, $v(t)$ and $\omega(t)$ are the UTV longitudinal and angular velocity, respectively, both considered to be the UTV control inputs. The uncertainties in the longitudinal and angular velocity, caused by unknown track friction, i.e. track slippage, are represented with $v_{\mathrm{d}}(t)$ and $\omega_{\mathrm{d}}(t)$, respectively.

Including the dynamic model of the UTV, the relation between the control inputs $v(t)$ and $\omega(t)$ and the angular velocities of the right and left track drive wheel $\Omega_{\mathrm{R}}(t)$ and $\Omega_{\mathrm{L}}(t)$, are given respectively as:

$$v(t) = \frac{r}{2}\left(\Omega_{\mathrm{R}}(t) + \Omega_{\mathrm{L}}(t)\right), \tag{2}$$

$$\omega(t) = \frac{r}{B}\left(\Omega_{\mathrm{R}}(t) - \Omega_{\mathrm{L}}(t)\right), \tag{3}$$

where r is the drive wheel radius and B is the normal distance between the right and left track.

In the presence of the track slippage, (2) and (3) can be modified respectively as:

$$v(t) + v_{\mathrm{d}}(t) = \frac{r}{2}\left(\Omega_{\mathrm{R}}(t) \cdot a_{\mathrm{R}}(t) + \Omega_{\mathrm{L}}(t) \cdot a_{\mathrm{L}}(t)\right), \tag{4}$$

$$\omega(t) + \omega_{\mathrm{d}}(t) = \frac{r}{B}\left(\Omega_{\mathrm{R}}(t) \cdot a_{\mathrm{R}}(t) - \Omega_{\mathrm{L}}(t) \cdot a_{\mathrm{L}}(t)\right), \tag{5}$$

where $a_{\mathrm{R}}(t)$ and $a_{\mathrm{L}}(t)$ are the unknown friction coefficients of the right and left track, which are in the range $[0, 1]$.

One can notice that the UTV motion control involves designing two control subsystems. The first one is for angular velocity control and involves a so-called lateral controller. The second subsystem is for longitudinal velocity control and deals with constructing a longitudinal controller.

Lateral controller design

To define the lateral control model, let us consider the UTV reference trajectory tracking problem shown in Figure 1, where the reference trajectory is defined by the kinematic model of a virtual target:

$$\begin{pmatrix} \dot{x}_{\mathrm{r}}(t) \\ \dot{y}_{\mathrm{r}}(t) \end{pmatrix} = \begin{pmatrix} \cos\theta_{\mathrm{r}}(t) \\ \sin\theta_{\mathrm{r}}(t) \end{pmatrix} \cdot \bar{v}_{\mathrm{r}}. \tag{6}$$

where $x_{\mathrm{r}}(t)$ and $y_{\mathrm{r}}(t)$ are the coordinates of the virtual target in the inertial coordinate system (X,Y), $\bar{v}_{\mathrm{r}} > 0$ is the virtual target longitudinal velocity and $\theta_{\mathrm{r}}(t)$ is the virtual target course angle. The path along track error $e_{\mathrm{s}}(t)$ and the cross-track error $e_{\mathrm{d}}(t)$ are defined in the vehicle coordinate system ($\mathrm{X_v}$, $\mathrm{Y_v}$) as:

$$\begin{pmatrix} e_{\mathrm{s}}(t) \\ e_{\mathrm{d}}(t) \end{pmatrix} = \begin{pmatrix} \cos\theta(t) & \sin\theta(t) \\ -\sin\theta(t) & \cos\theta(t) \end{pmatrix} \cdot \begin{pmatrix} x_{\mathrm{r}}(t) - x(t) \\ y_{\mathrm{r}}(t) - y(t) \end{pmatrix}. \tag{7}$$

By denoting the course angle error as:

$$\theta_{\mathrm{e}}(t) = \theta(t) - \theta_{\mathrm{r}}(t), \tag{8}$$

and substituting (1) and (6) in the derivative of (7), one can obtain trajectory tracking and course angle errors dynamics as:

$$\begin{aligned} \dot{e}_{\mathrm{s}}(t) &= \dot{\theta}(t) \cdot e_{\mathrm{d}}(t) - v(t) - v_{\mathrm{d}}(t) + \bar{v}_{\mathrm{r}} \cos\theta_{\mathrm{e}}(t), \\ \dot{e}_{\mathrm{d}}(t) &= \bar{v}_{\mathrm{r}} \sin\theta_{\mathrm{e}}(t) - \dot{\theta}(t) \cdot e_{\mathrm{s}}(t), \\ \dot{\theta}_{\mathrm{e}}(t) &= \omega(t) + \omega_{\mathrm{d}}(t) - \dot{\theta}_{\mathrm{r}}(t). \end{aligned} \tag{9}$$

As in practice, the cross-track error is the main concern (Chen et al., 2019). To facilitate that, the lateral control subsystem can be formulated from (9) as:

$$\dot{e}_{\mathrm{d}}(t) = \bar{v}_{\mathrm{r}} \sin\theta_{\mathrm{e}}(t) + d_1(t), \tag{10}$$

$$\dot{\theta}_{\mathrm{e}}(t) = \omega(t) + d_2(t), \tag{11}$$

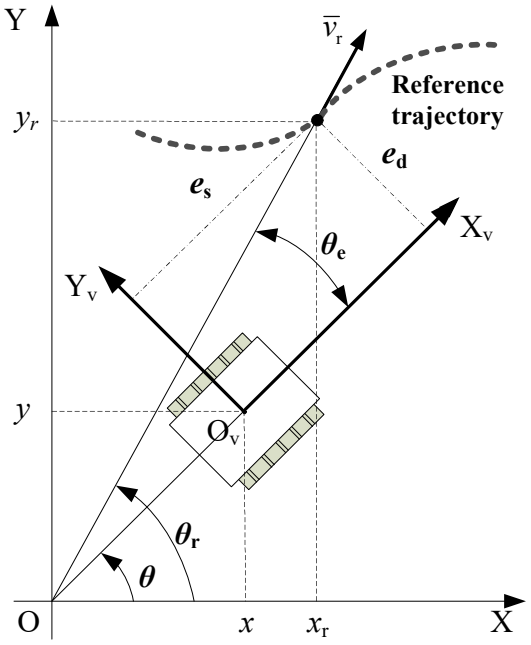

Figure 1 – Considered UTV trajectory tracking problem

with $d_1(t) = \dot{\theta}(t) \cdot e_s(t)$ and $d_2(t) = \omega_d(t) + \dot{\theta}_r(t)$, which represents collectively the disturbances caused by slippage, reference trajectory dynamics, and longitudinal channel coupling (reflected in the influence of the $v(t)$ on the lateral controller).

By substituting (11) in the derivative of (10), the cross-track error dynamics can be presented in a compact ADRC form as:

$$\ddot{e}_d(t) = b_0 \cdot \omega(t) + f_l(t), \tag{12}$$

where $b_0 = \bar{v}_r$ is the known part of the lateral model and $f_l(t) = \bar{v}_r(\cos\theta_e(t) - 1) \cdot \omega(t) + \bar{v}_r \cos\theta_e(t) \cdot d_2(t) + \dot{d}_1(t)$ is denoted as the total disturbance of the lateral control subsystem. One can see that the lateral control is formulated as a regulation problem, where the error signal $e_d(t)$ has to be minimized by manipulating the control input $\omega(t)$, all in the presence of perturbing effects like slippage disturbances, coupling dynamics with the longitudinal channel, and the reference trajectory dynamics.

To design the ADRC controller, model (12) is expressed as a following extended state-space model:

$$\begin{pmatrix} \dot{e}_{\mathrm{d}}(t) \\ \ddot{e}_{\mathrm{d}}(t) \\ \dot{f}_{\mathrm{l}}(t) \end{pmatrix} = \begin{pmatrix} 0 & 1 & 0 \\ 0 & 0 & 1 \\ 0 & 0 & 0 \end{pmatrix} \cdot \begin{pmatrix} e_{\mathrm{d}}(t) \\ \dot{e}_{\mathrm{d}}(t) \\ f_{\mathrm{l}}(t) \end{pmatrix} + \begin{pmatrix} 0 \\ b_0 \\ 0 \end{pmatrix} \cdot \omega(t) + \begin{pmatrix} 0 \\ 0 \\ 1 \end{pmatrix} \cdot \dot{f}_{\mathrm{l}}(t), \tag{13}$$

and the states can be estimated by an appropriate observer, for example, a linear ESO shown in (Łakomy et al., 2020):

$$\begin{pmatrix} \dot{\hat{e}}_{\mathrm{d}}(t) \\ \ddot{\hat{e}}_{\mathrm{d}}(t) \\ \dot{\hat{f}}_{\mathrm{l}}(t) \end{pmatrix} = \begin{pmatrix} 0 & 1 & 0 \\ 0 & 0 & 1 \\ 0 & 0 & 0 \end{pmatrix} \cdot \begin{pmatrix} \hat{e}_{\mathrm{d}}(t) \\ \dot{\hat{e}}_{\mathrm{d}}(t) \\ \hat{f}_{\mathrm{l}}(t) \end{pmatrix} + \begin{pmatrix} 0 \\ b_0 \\ 0 \end{pmatrix} \cdot \omega(t) + \begin{pmatrix} l_{\mathrm{l}1} \\ l_{\mathrm{l}2} \\ l_{\mathrm{l}3} \end{pmatrix} \cdot \left(e_{\mathrm{d}}(t) - \hat{e}_{\mathrm{d}}(t) \right), \tag{14}$$

where $l_{\mathrm{l}1}$, $l_{\mathrm{l}2}$, and $l_{\mathrm{l}3}$ are the observer gains, which can be relatively simply tuned by the *bandwidth parameterization* from (Gao, 2003) by placing observer poles at the same location $\lambda = -\omega_{\mathrm{ESO_l}}$:

$$(\lambda + \omega_{\mathrm{ESO_l}})^3 \stackrel{!}{=} \lambda^3 + l_{\mathrm{l}1} \cdot \lambda^2 + l_{\mathrm{l}2} \cdot \lambda + l_{\mathrm{l}3}, \tag{15}$$

where $\omega_{\mathrm{ESO_l}}$ is the desired observer bandwidth.

By assuming $\theta_{\mathrm{e}}(t) \in \{-\pi, \pi\}$, the saturated lateral control law can be proposed as:

$$\omega(t) = \begin{cases} \omega_{\max} \cdot \mathrm{sat}\left(u_{\mathrm{l}}(t)/\omega_{\max} \right), & \text{when} \quad |\theta_{\mathrm{e}}(t)| < \frac{\pi}{2} \\ \omega_{\max}, & \text{when} \quad \frac{\pi}{2} \leq \theta_{\mathrm{e}}(t) < \pi \\ -\omega_{\max}, & \text{when} \quad -\pi < \theta_{\mathrm{e}}(t) \leq -\frac{\pi}{2} \end{cases} \tag{16}$$

where $\mathrm{sat}(a) = \min\left(1, |a|\right) \cdot \mathrm{sign}(a)$ is a saturation function, $\omega_{\max} > 0$ is saturation level of the lateral ADRC signal, denoted as:

$$u_{\mathrm{l}}(t) = \frac{1}{b_0} \left(-k_{\mathrm{pl}} \cdot \hat{e}_{\mathrm{d}}(t) - k_{\mathrm{dl}} \cdot \dot{\hat{e}}_{\mathrm{d}}(t) - \hat{f}_{\mathrm{l}}(t) \right), \tag{17}$$

with the controller design parameters k_{pl} and k_{dl}. The saturation $\omega_{\max}$ is introduced to reduce slippage caused by the large centrifugal force, i.e. the high value of the UTV angular acceleration, as discussed in (Lu et al.,

2016). It should be also noted that control law (16) is designed to enable quick reduction of the course angle error in the range $\theta_{\mathrm{e}}(t) \in \{-\pi/2, \pi/2\}$ and to avoid the control signal (17) saturation.

Now, by assuming $f_{\mathrm{l}}(t) \approx \hat{f}_{\mathrm{l}}(t)$, $\dot{e}_{\mathrm{d}}(t) \approx \hat{\dot{e}}_{\mathrm{d}}(t)$, $e_{\mathrm{d}}(t) \approx \hat{e}_{\mathrm{d}}(t)$ and substituting (16) in (12), the following relation can take place:

$$\ddot{e}_{\mathrm{d}}(t) + k_{\mathrm{dl}} \cdot \dot{e}_{\mathrm{d}}(t) + k_{\mathrm{pl}} \cdot e_{\mathrm{d}}(t) \approx 0. \tag{18}$$

From (18) one can see that the lateral control performances can be adjusted by appropriately selecting the parameters k_{pl} and k_{dl}. Applying the already mentioned *bandwidth parameterization*, the controller parameters can be tuned by placing closed-loop controller poles at the common location $\lambda = -\omega_{\mathrm{CL_l}}$:

$$(\lambda + \omega_{\mathrm{CL_l}})^2 \stackrel{!}{=} \lambda^2 + k_{\mathrm{dl}} \cdot \lambda + k_{\mathrm{pl}}, \tag{19}$$

where $\omega_{\mathrm{CL_l}}$ is the desired closed-loop lateral control system bandwidth.

Longitudinal controller design

Let us denote the UTV longitudinal velocity in the presence of slippage disturbance as $v_{\mathrm{v}}(t) = v(t) + v_{\mathrm{d}}(t)$. Thus, the longitudinal velocity control model can be formulated as:

$$\dot{v}_{\mathrm{v}}(t) = u_{\mathrm{v}}(t) + \dot{v}_{\mathrm{d}}(t), \tag{20}$$

where $u_{\mathrm{v}}(t) = \dot{v}(t)$ represents the control signal which should be designed to make $v_{\mathrm{v}}(t)$ track the reference target longitudinal velocity $\bar{v}_{\mathrm{r}}$ even in the presence of the disturbance $v_{\mathrm{d}}(t)$. To apply the ADRC concept to the considered problem, system (20) can be rewritten in the extended state-space form as:

$$\begin{pmatrix} \dot{v}_{\mathrm{v}}(t) \\ \dot{f}_{\mathrm{v}}(t) \end{pmatrix} = \begin{pmatrix} 0 & 1 \\ 0 & 0 \end{pmatrix} \cdot \begin{pmatrix} v_{\mathrm{v}}(t) \\ f_{\mathrm{v}}(t) \end{pmatrix} + \begin{pmatrix} 1 \\ 0 \end{pmatrix} \cdot u_{\mathrm{v}}(t) + \begin{pmatrix} 0 \\ 1 \end{pmatrix} \cdot \dot{f}_{\mathrm{v}}(t), \tag{21}$$

where $f_{\mathrm{v}}(t) = \dot{v}_{\mathrm{d}}(t)$ is the longitudinal channel total disturbance, which can be estimated by an appropriately constructed ESO:

$$\begin{pmatrix} \hat{\dot{v}}_{\mathrm{v}}(t) \\ \hat{\dot{f}}_{\mathrm{v}}(t) \end{pmatrix} = \begin{pmatrix} 0 & 1 \\ 0 & 0 \end{pmatrix} \cdot \begin{pmatrix} \hat{v}_{\mathrm{v}}(t) \\ \hat{f}_{\mathrm{v}}(t) \end{pmatrix} + \begin{pmatrix} 1 \\ 0 \end{pmatrix} \cdot u_{\mathrm{v}}(t) + \begin{pmatrix} l_{\mathrm{v1}} \\ l_{\mathrm{v2}} \end{pmatrix} \cdot \left(v_{\mathrm{v}}(t) - \hat{v}_{\mathrm{v}}(t)\right), \tag{22}$$

where $l_{\mathrm{v}1}$ and $l_{\mathrm{v}2}$ are the observer gains. As in the previously shown lateral control channel, the active rejection of the total disturbance $f_{\mathrm{v}}(t)$ can be realized using its estimation $\hat{f}_{\mathrm{v}}(t)$ by applying the following ADRC governing law:

$$u_{\mathrm{v}}(t) = k_{\mathrm{pv}}\left(\bar{v}_{\mathrm{r}} - v_{\mathrm{v}}(t)\right) - \hat{f}_{\mathrm{v}}(t), \tag{23}$$

where k_{pv} is an adjustable controller parameter. Assuming $f_{\mathrm{v}}(t) \approx \hat{f}_{\mathrm{v}}(t)$ and substituting (23) into (20) results in:

$$\dot{v}_{\mathrm{v}}(t) + k_{\mathrm{pv}} \cdot v_{\mathrm{v}}(t) \approx k_{\mathrm{pv}} \cdot \bar{v}_{\mathrm{r}}, \tag{24}$$

where one can see that the desired control performances can be obtained by an appropriate selection of the parameter k_{pv}.

In the same manner, as in the lateral control subsystem, the longitudinal ESO and controller gains can be tuned by utilizing the *bandwidth parameterization* methodology, i.e.:

$$(\lambda + \omega_{\mathrm{ESO_v}})^2 \stackrel{!}{=} \lambda^2 + l_{\mathrm{v}1} \cdot \lambda + l_{\mathrm{v}2}, \tag{25}$$

$$\lambda + \omega_{\mathrm{CL_v}} \stackrel{!}{=} \lambda + k_{\mathrm{pv}}, \tag{26}$$

where $\omega_{\mathrm{ESO_v}}$ and $\omega_{\mathrm{CL_v}}$ are the desired longitudinal ESO bandwidth and the longitudinal closed-loop control system bandwidth, respectively.

A schematic representation of the UTV control architecture, based on the proposed ADRC lateral and longitudinal controllers, is shown in Figure 2.

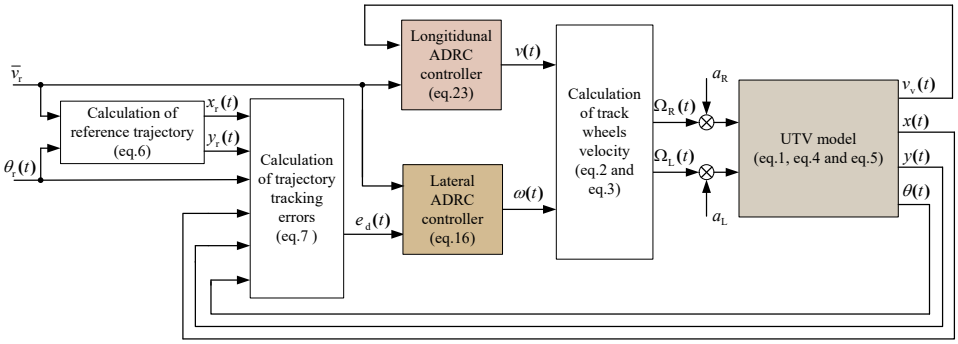

Figure 2 – The proposed UTV control architecture

Control system verification

Since the hardware implementation of the control algorithm requires its discrete form, simulation experiments are carried out with a discrete-time version of the proposed UTV controllers. Therefore, the discretization of the lateral and longitudinal controllers is presented first, followed by simulation results.

Simulation validation

Since the lateral and the longitudinal ADRC control laws (17) and (23) are in linear forms, only the observer need to be discretized. To enhance the closed-loop system stability for a low sampling rate T_s, the current discrete models from (Miklosovic et al., 2006; Herbst & Madonski, 2023) are used. Therefore, for the lateral ESO (14), its discrete form is defined as:

$$\begin{pmatrix} \hat{e}_{\mathrm{d}}(k) \\ \hat{\dot{e}}_{\mathrm{d}}(k) \\ \hat{\dot{f}}_{\mathrm{l}}(k) \end{pmatrix} = \left(A_{\mathrm{dl}} - L_{\mathrm{cl}} \cdot C_{\mathrm{dl}} \cdot A_{\mathrm{dl}}\right) \cdot \begin{pmatrix} \hat{e}_{\mathrm{d}}(k-1) \\ \hat{\dot{e}}_{\mathrm{d}}(k-1) \\ \hat{\dot{f}}_{\mathrm{l}}(k-1) \end{pmatrix} + \left(B_{\mathrm{dl}} - L_{\mathrm{cl}} \cdot C_{\mathrm{dl}} \cdot B_{\mathrm{dl}}\right) \cdot \omega(k-1) + L_{\mathrm{cl}} \cdot e_{\mathrm{d}}(k), \tag{27}$$

where:

$$A_{\mathrm{dl}} = \begin{pmatrix} 1 & T_s & T_s^2/2 \\ 0 & 1 & T_s \\ 0 & 0 & 1 \end{pmatrix}, B_{\mathrm{dl}} = \begin{pmatrix} b_0 \cdot T_s^2/2 \\ b_0 \cdot T_s \\ 0 \end{pmatrix}, C_{\mathrm{dl}} = \begin{pmatrix} 1 & 0 & 0 \end{pmatrix},$$

are the discrete observer matrices obtained by applying the zero-order hold (ZOH) discretization method from (Miklosovic et al., 2006). The discrete ESO gains vector L_{cl} is computed by placing the discrete observer poles in one location $\beta = e^{-\omega_{\mathrm{ESO_l}} T_s}$,i.e.:

$$|zI - (A_{\mathrm{dl}} - A_{\mathrm{dl}} \cdot L_{\mathrm{cl}} \cdot C_{\mathrm{dl}})| \stackrel{!}{=} (z - \beta)^3.$$

In the same manner, the discrete-time model of the longitudinal controller ESO (22) is obtained as:

$$\begin{pmatrix} \hat{\dot{v}}_{\mathrm{v}}(k) \\ \hat{\dot{f}}_{\mathrm{v}}(k) \end{pmatrix} = \left(A_{\mathrm{dv}} - L_{\mathrm{cv}} \cdot C_{\mathrm{dv}} \cdot A_{\mathrm{dv}}\right) \cdot \begin{pmatrix} \hat{v}_{\mathrm{v}}(k-1) \\ \hat{f}_{\mathrm{v}}(k-1) \end{pmatrix}$$

$$+\left(B_{\mathrm{dv}}-L_{\mathrm{cv}}\cdot C_{\mathrm{dv}}\cdot B_{dv}\right)\cdot u_{\mathrm{v}}(k-1)+L_{\mathrm{cv}}\cdot v_{\mathrm{v}}(k), \tag{28}$$

where:

$$A_{\mathrm{dv}}=\begin{pmatrix}1 & T_s\\ 0 & 1\end{pmatrix}, B_{\mathrm{dv}}=\begin{pmatrix}b_0\cdot T_s\\ 0\end{pmatrix}, C_{\mathrm{dv}}=\begin{pmatrix}1 & 0\end{pmatrix},$$

are the matrices determined by the ZOH discretization. The longitudinal discrete ESO gains vector L_{cv} is computed by placing discrete observer poles in the location $\beta=e^{-\omega_{\mathrm{ESO_v}}T_s}$, i.e.:

$$|zI-(A_{\mathrm{dv}}-A_{\mathrm{dv}}\cdot L_{\mathrm{cv}}\cdot C_{\mathrm{dv}})|\stackrel{!}{=}(z-\beta)^2.$$

The simulation experiments are conducted in MATLAB/Simulink using the model of the laboratory skid-steer UTV, with dimensions $r=0.3\,\mathrm{m}$ and $B=0.7\,\mathrm{m}$. To demonstrate the effectiveness of the proposed ADRC algorithm, its performance is compared with the UTV control architecture realized by the standard industrial discrete PID controller with a noise filter in the lateral control subsystem and the PI controller in the longitudinal control subsystem. To make the test more realistic, the maximal UTV angular velocity is limited to $\omega_{\max}=2\cdot\pi\,\mathrm{rad/s}$. The reference trajectory is defined using the kinematic model (6), with $\bar{v}_{\mathrm{r}}=2\,\mathrm{m/s}$ and:

$$\theta_{\mathrm{r}}(k\cdot T_s)=\begin{cases}0.05\cdot k\cdot T_s, & \text{when}\quad 0\,\mathrm{s}<k\cdot T_s\leq 8\,\mathrm{s};\\ -0.1\cdot k\cdot T_s, & \text{when}\quad 8\,\mathrm{s}<k\cdot T_s\leq 16\,\mathrm{s};\\ -0.05\cdot k\cdot T_s, & \text{when}\quad 16\,\mathrm{s}<k\cdot T_s\leq 22\,\mathrm{s};\\ 0.15\cdot k\cdot T_s, & \text{when}\quad 22\,\mathrm{s}<k\cdot T_s\leq 35\,\mathrm{s}.\end{cases} \tag{29}$$

The simulations are realized through the following two cases.

Simulation case #1

In this case, it is assumed that the UTV is not affected by the slippage disturbances ($a_{\mathrm{R}}=1$ and $a_{\mathrm{L}}=1$). Both of the considered control approaches (the proposed ADRC and the standard PI/PID) were tuned empirically with the goal to enable similar control performances in terms of minimization of the cross-track error e_{d}. Therefore, in the lateral PID controller, four parameters: proportional, integral, and derivative gains, as well as the noise filter coefficient, are set as $k_{\mathrm{P_l}}=4.5$, $k_{\mathrm{I_l}}=1$, $k_{\mathrm{D_l}}=0.5$ and $N=85$, and the proportional and integral gains of the longitudinal PI controller are set as $k_{\mathrm{P_v}}=1.5$, $k_{\mathrm{I_v}}=0.1$. The ADRC control structure is tuned

by choosing $\omega_{\mathrm{CL_l}} = 1\,$rad/s and $\omega_{\mathrm{ESO_l}} = 10\,$rad/s for the lateral controller, and $\omega_{\mathrm{CL_v}} = 1.4\,$rad/s and $\omega_{\mathrm{ESO_v}} = 16\,$rad/s for the longitudinal controller. Both systems are discretized with the same sampling time $T_s = 20\,$ms. The obtained results of the reference trajectory tracking performances, including cross-track errors, longitudinal velocities, and drive wheels velocities are depicted in Figure 3.

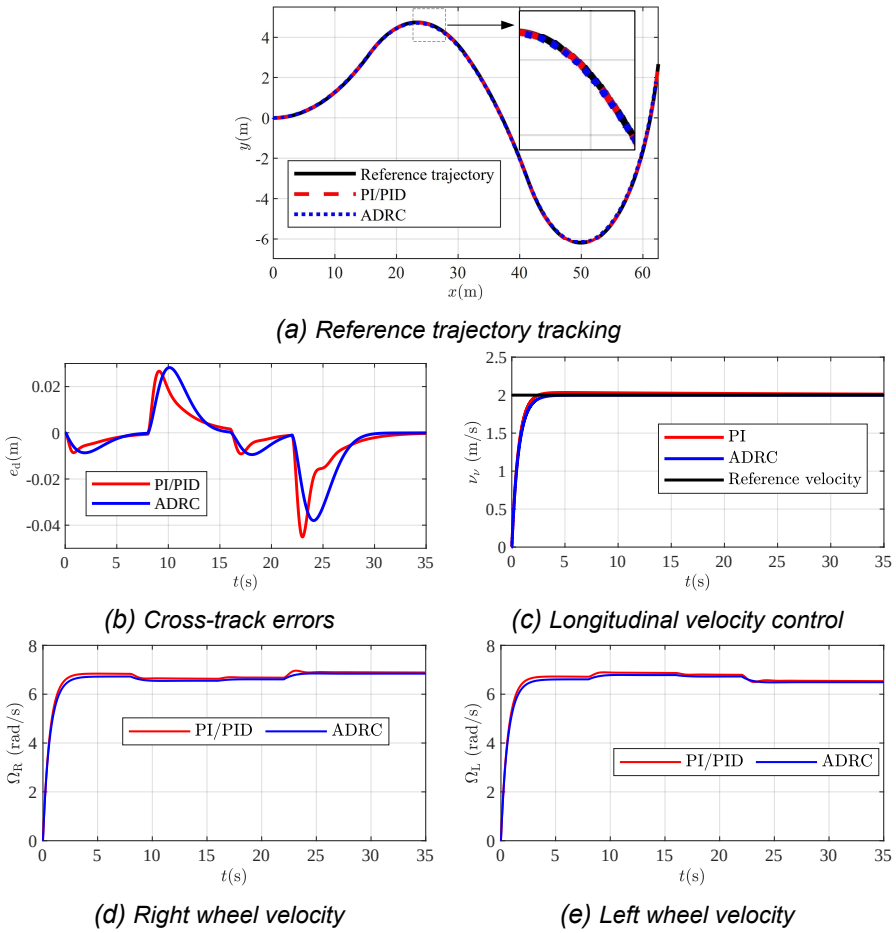

(a) Reference trajectory tracking

(b) Cross-track errors

(c) Longitudinal velocity control

(d) Right wheel velocity

(e) Left wheel velocity

Figure 3 – Simulation results for simulation case #1

In accordance with the set goal of this simulation case, one can see that both control approaches provide effective tracking of the reference trajectory, with similar values of the cross-track errors peaks that occur when $\theta_{\mathrm{r}}(t)$ changes the value (see (29)). The drive wheels velocities are bounded

and smooth for both systems, and it can be seen that the PI/PID algorithms generate slightly larger values.

Simulation case #2

In this case, the controllers have kept the settings from the previous one. The slippage disturbances with dynamics $a_{\mathrm{R}} = 0.7 + 0.3\sin(2 \cdot k \cdot T_s)$ and $a_{\mathrm{L}} = 0.7 + 0.3\sin(4 \cdot k \cdot T_s)$, which simulate vehicle motion over uneven dirt terrains, are included from $t = 10\,\mathrm{s}$.

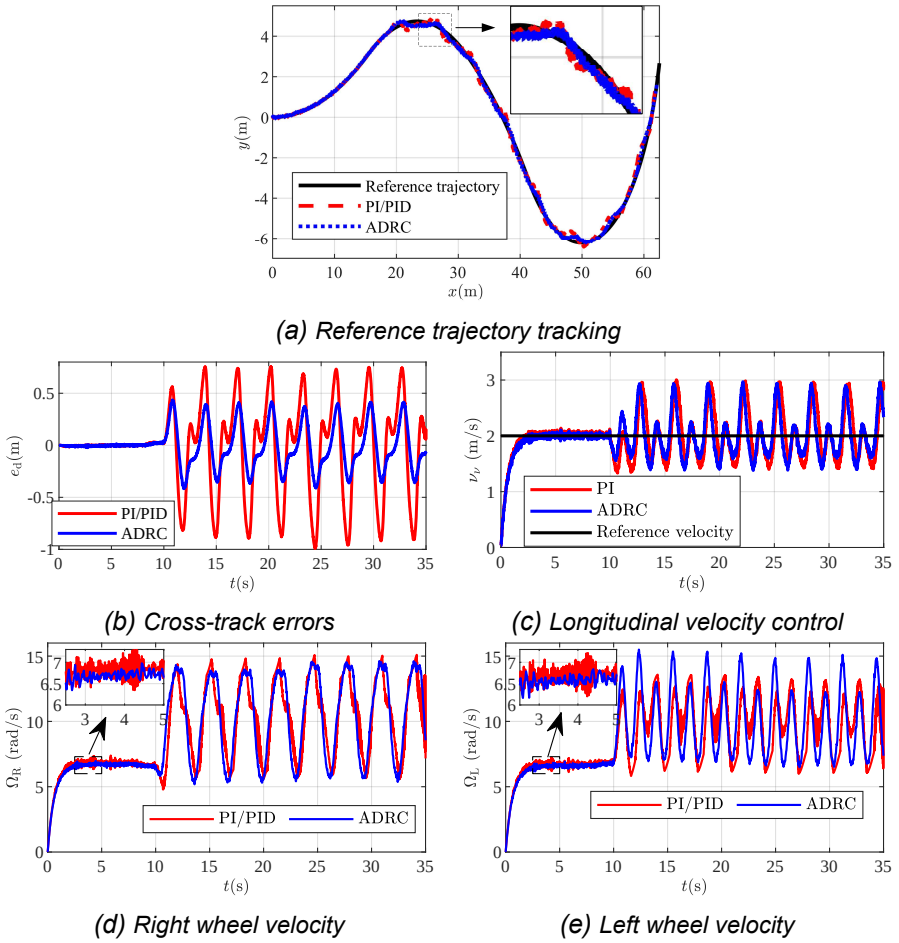

(a) Reference trajectory tracking

(b) Cross-track errors

(c) Longitudinal velocity control

(d) Right wheel velocity

(e) Left wheel velocity

Figure 4 – Simulation results for simulation case #2

Also, the measurement errors of the UTV position (x, y), the angle orientation (θ), and the longitudinal velocity (v_v) are modeled as Gaussian noises with zero means and standard deviations [0.1 m, 0.1 m, 0.01 rad, 0.1 m/s], respectively. It corresponds with the errors of the GPS and inertial sensors in the real vehicle. The reference trajectory tracking performances and drive wheel velocities comparisons of PI/PID and ADRC are shown in Figure 4. It is noticeable that in the presence of the slippage dynamics, ADRC enables better tracking performances, with significantly lower values of the cross-track error peaks. In addition, it can be noted that the added measurement errors caused ruggedness in drive wheel velocities. However, from the zoomed part of Figure 4d and Figure 4e, it is evident that ADRC generates more smooth drive wheels velocities than the PI/PID algorithm, which is important for practical implementation.

FPGA-in-the-loop simulation validation

In order to analyze the challenges of the practical implementation, the FIL (FPGA-in-the-loop) simulation with the proposed ADRC-based UTV control is carried out. Such a validation method reduces the gap between pure simulation design (which may be too idealized) and implementation on the real vehicle (which may be time-consuming). To this end, a hardware description language code of the discrete lateral and longitudinal controllers is generated in the fixed-point word-length (WL) format, for the signals and coefficients representations, and implemented in FPGA board Basys 3 with Xilinx chip XC7A35T. By connecting JTAG port of the FPGA board and the personal computer USB port, the FIL simulations are executed by exchanging signals between the UTV model, defined in MATLAB/Simulink, and the controllers, implemented in the FPGA chip. The graphical structure of the FIL simulation methodology is demonstrated in Figure 5.

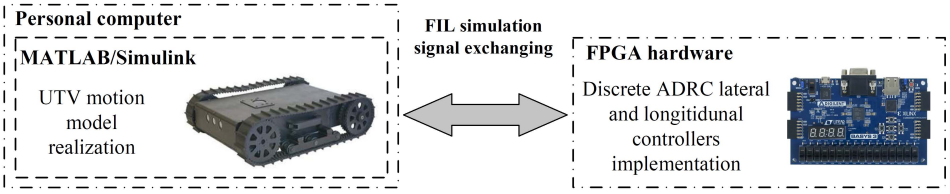

Figure 5 – FIL validation methodology

The FIL simulations are performed with the setup as in simulation case #2. The reference trajectory and longitudinal velocity tracking performances, for the ADRC algorithm implemented in the fixed-point format with WLs of 24, 22, and 20 bits, are compared with the pure MATLAB/Simulink simulation results (shown in simulation case #2) and gathered in Figure 6.

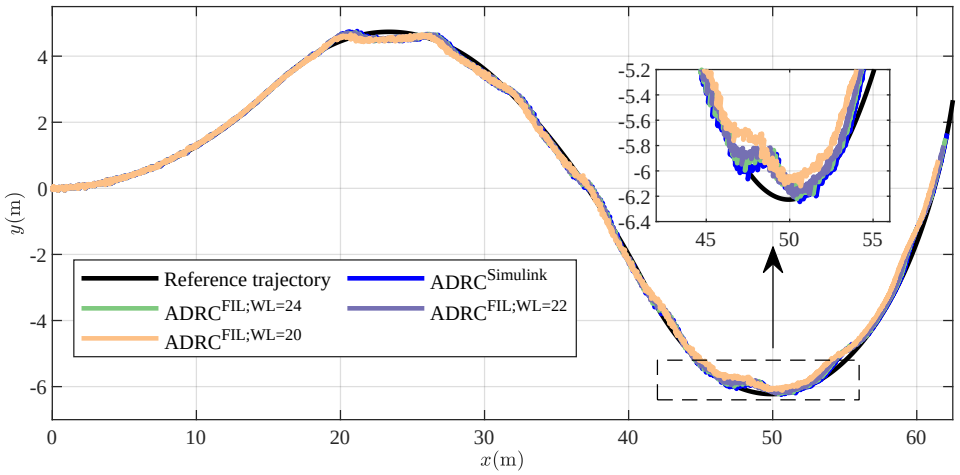

(a) Reference trajectory tracking

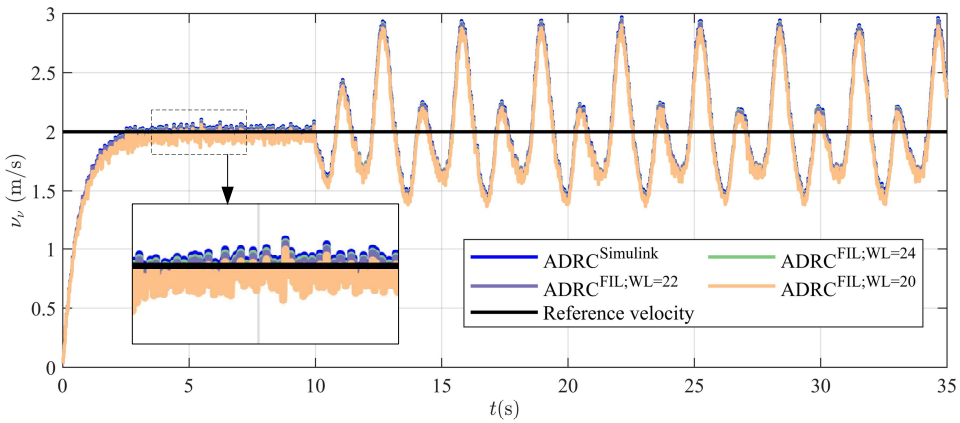

(b) Longitudinal velocity control

Figure 6 – FIL simulation reference trajectory tracking results

In order to make the impact of the fixed-point format quantization error (QE) more visible, the differences in cross-track errors, between the pure MATLAB/Simulink simulation and the appropriate FIL simulations, denoted

as $e_{\mathrm{d}}^{\mathrm{QE}}$, are shown in Figure 7. The obtained drive wheels velocities are shown in Figure 8. In addition, the appropriate FPGA resource occupancy values, for different values of WLs, are shown in Table 1.

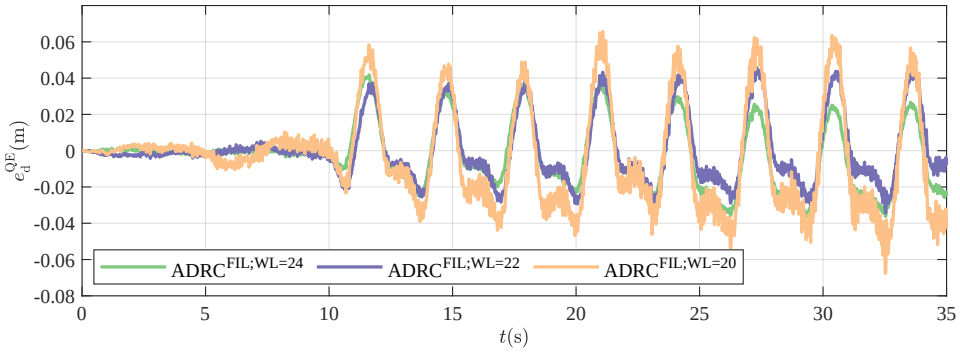

Figure 7 – The difference in the cross-track error between the Simulink simulation and the FIL simulations with the appropriate WL of the fixed-point format

Table 1 – Resource occupancy of FPGA chip XC7A35T for the fixed-point ADRC controllers implementation with different WLs

FPGA resource	WL = 24	WL = 22	WL = 20	Available
LUTs	5433 (26.2%)	4821 (23.2%)	4441(21.3%)	20800 (100%)
FF blocks	545 (1.3%)	525 (1.2%)	499(1.2%)	41600 (100%)
DSP blocks	82 (91%)	81 (90%)	78 (87%)	90 (100%)

As it can be seen, the FIL simulation results are close to the simulation results, which confirms the high performances of the FPGA-based implementation of the lateral and longitudinal ADRC controllers. As expected, the slight performance degradation occurs with the decrease of WL, i.e. with lower precision of the signals and coefficients in the implemented controllers. Although increasing WL requires more FPGA resource occupancy, from Table 1 one can see that it is not a significant increase that enables the realization of a high-precision fixed-point ADRC implementation on low-cost FPGA chip, such as XC7A35T.

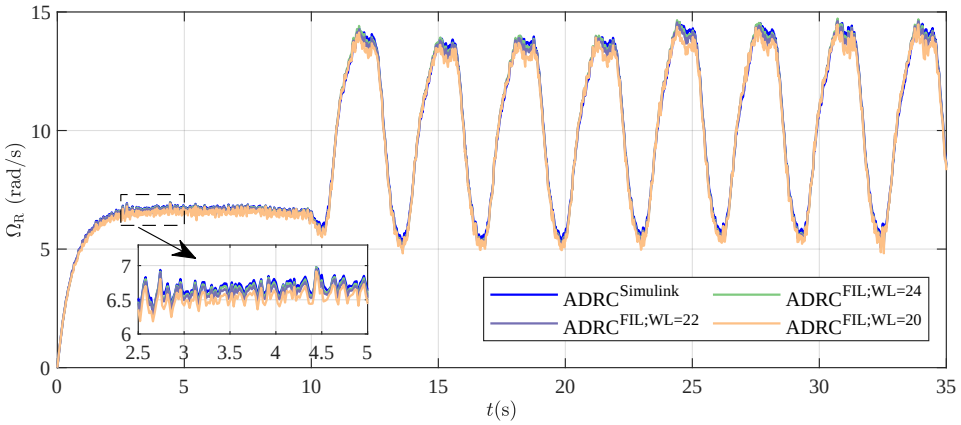

(a) Right wheel velocity

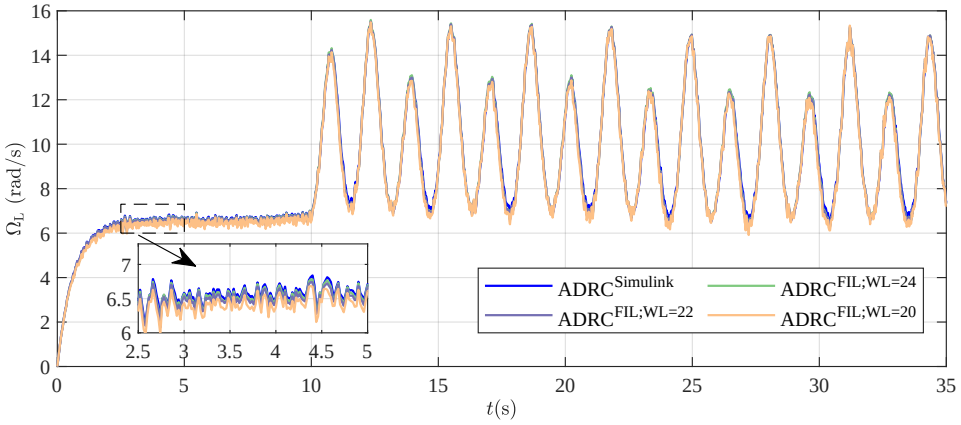

(b) Left wheel velocity

Figure 8 – FIL simulation drive wheel velocities

Conclusion

To improve the UTV trajectory tracking performances, the systematic use of an ADRC-based control structure was suggested in this research. The slippage disturbances and the internal UTV model uncertainties were treated collectively as lumped (total) disturbances in the lateral and longitudinal control channels. The efficiency of the proposed ADRC approach was illustrated in comparison with the classical PI/PID control, through the typical UTV trajectory tracking simulation scenarios.

Additionally, the FIL simulation was used to experimentally validate the fixed-point FPGA implementation of the proposed lateral and longitudinal ADRC controllers. The conducted applied research has validated the efficacy of the proposed systematic procedure of applying the ADRC methodology for the specific UTV trajectory tracking problem, which includes its design, tuning, FPGA implementation, and performance verification.

References

Al-Jarrah, A., Salah, M. & Almomani, F. 2019. Controlling a Skid-Steered Tracked Mobile Robot with Slippage Using Various Control Schemes. In: *2019 20th International Conference on Research and Education in Mechatronics (REM)*. Wels, Austria, pp.1-7, May 23-24. Available at: https://doi.org/10.1109/REM.2019.8744123.

Burke, M. 2012. Path-following control of a velocity constrained tracked vehicle incorporating adaptive slip estimation. In: *2012 IEEE International Conference on Robotics and Automation*. Saint Paul, MN, USA, pp.97-102, May 14-18. Available at: https://doi.org/10.1109/ICRA.2012.6224684.

Chen, S., Xue, W., Lin, Z. & Huang, Y. 2019. On Active Disturbance Rejection Control for Path Following of Automated Guided Vehicle with Uncertain Velocities. In: *2019 American Control Conference (ACC)*. Philadelphia, PA, USA, pp.2446-2451, July 10-12. Available at: https://doi.org/10.23919/ACC.2019.8815348.

Dai, Y., Zhu, X., Zhou, H., Mao, Z. & Wu, W. 2018. Trajectory Tracking Control for Seafloor Tracked Vehicle By Adaptive Neural-Fuzzy Inference System Algorithm. *International Journal of Computers Communications & Control*, 13(4), pp. 465–476 [online]. Available at: https://www.univagora.ro/jour/index.php/ijccc/article/view/3267 [Accessed: 20 March 2024].

De Luca, A., Oriolo, G. & Samson, C. 1998. Feedback control of a nonholonomic car-like robot. In: *Laumond, J.P. (Ed.) Robot Motion Planning and Control. Lecture Notes in Control and Information Sciences*. 229, pp.171-253. Berlin, Heidelberg: Springer. Available at: https://doi.org/10.1007/BFb0036073.

Gao, Z. 2003. Scaling and bandwidth-parameterization based controller tuning. In: *Proceedings of the 2003 American Control Conference*. Denver, CO, USA, pp.4989-4996, June 04-06. Available at: https://doi.org/10.1109/ACC.2003.1242516.

Gao, Z. 2006. Active disturbance rejection control: a paradigm shift in feedback control system design. In: *2006 American Control Conference*. Minneapolis, MN, USA, p.7, June 14-16. Available at: https://doi.org/10.1109/ACC.2006.1656579.

Gonzalez, R., Fiacchini, M., Alamo, T., Guzman, J.L. & Rodriguez, F. 2010. Adaptive Control for a Mobile Robot Under Slip Conditions Using an LMI-Based Approach. *European Journal of Control*, 16(2), pp. 144–155. Available at: https://doi.org/10.3166/ejc.16.144-155.

Herbst, G. & Madonski, R. 2023. Tuning and implementation variants of discrete-time ADRC. *Control Theory and Technology*, 21, pp. 72–88. Available at: https://doi.org/10.1007/s11768-023-00127-0.

Hiramatsu, T., Morita, S., Pencelli, M., Niccolini, M., Ragaglia, M. & Argiolas, A. 2019. Path-Tracking Controller for Tracked Mobile Robot on Rough Terrain. *International Journal of Electrical and Computer Engineering*, 13(2), pp. 59–64. Available at: https://doi.org/10.5281/zenodo.2571922.

Hong, S., Choi, J.S., Kim, H.W., Won, M.C., Shin, S.C., Rhee, J.S. & Park, H.u. 2009. A path tracking control algorithm for underwater mining vehicles. *Journal of Mechanical Science and Technology*, 23(8), pp. 2030–2037.

Hu, J., Tao, J., Zhao, W. & Han, Y. 2019. Modeling and simulation of steering control strategy for dual-motor coupling drive tracked vehicle. *Journal of the Brazilian Society of Mechanical Sciences and Engineering*, 41, art.number:190. Available at: https://doi.org/10.1007/s40430-019-1692-0.

Huang, H., Zhai, L. & Wang, Z. 2018a. A Power Coupling System for Electric Tracked Vehicles during High-Speed Steering with Optimization-Based Torque Distribution Control. *Energies*, 11(6), art.number:1538. Available at: https://doi.org/10.3390/en11061538.

Huang, P., Zhang, Z., Luo, X., Zhang, J. & Huang, P. 2018b. Path Tracking Control of a Differential-Drive Tracked Robot Based on Look-ahead Distance. *IFAC-PapersOnLine*, 51(17), pp. 112–117. Available at: https://doi.org/10.1016/j.ifacol.2018.08.072.

Janarthanan, B., Padmanabhan, C. & Sujatha, C. 2012. Longitudinal dynamics of a tracked vehicle: Simulation and experiment. *Journal of Terramechanics*, 49(2), pp. 63–72. Available at: https://doi.org/10.1016/j.jterra.2011.11.001.

Łakomy, K., Patelski, R. & Pazderski, D. 2020. ESO Architectures in the Trajectory Tracking ADR Controller for a Mechanical System: A Comparison. In: *Bartoszewicz, A., Kabziński, J. & Kacprzyk, J. (Eds.) Advanced, Contemporary Control*. 1196, pp.1323–1335. Cham: Springer. Available at: https://doi.org/10.1007/978-3-030-50936-1_110.

Li, Y., Yu, J., Guo, X. & Sun, J. 2020. Path Tracking Method Of Unmanned Agricultural Vehicle Based On Compound Fuzzy Control. In: *IEEE 9th Joint International Information Technology and Artificial Intelligence Conference (ITAIC)*. Chongqing, China, pp.1301-1305, December 11-13. Available at: https://doi.org/10.1109/ITAIC49862.2020.9338981.

Lu, H., Xiong, G. & Guo, K. 2016. Motion Predicting of Autonomous Tracked Vehicles with Online Slip Model Identification. *Mathematical Problems in Engineering*, 2016(1), art.number:6375652. Available at: https://doi.org/10.1155/2016/6375652.

Miklosovic, R., Radke, A. & Gao, Z. 2006. Discrete implementation and generalization of the extended state observer. In: *2006 American Control Conference*. Minneapolis, MN, USA, p.6, June 14-16. Available at: https://doi.org/10.1109/ACC.2006.1656547.

Mitsuhashi, T., Chida, Y. & Tanemura, M. 2019. Autonomous Travel of Lettuce Harvester using Model Predictive Control. *IFAC-PapersOnLine*, 52(30), pp. 155–160. Available at: https://doi.org/10.1016/j.ifacol.2019.12.514.

Nonami, K., Kartidjo, M., Yoon, K.J. & Budiyono, A. 2013. *Autonomous Control Systems and Vehicles, Intelligent Unmanned Systems*. Tokyo: Springer. Available at: https://doi.org/10.1007/978-4-431-54276-6.

Pentzer, J., Brennan, S. & Reichard, K. 2014. Model-based Prediction of Skid-steer Robot Kinematics Using Online Estimation of Track Instantaneous Centers of Rotation. *Journal of Field Robotics*, 31(3), pp. 455–476. Available at: https://doi.org/10.1002/rob.21509.

Sabiha, A.D., Kamel, M.A., Said, E. & Hussein, W.M. 2022. ROS-based trajectory tracking control for autonomous tracked vehicle using optimized backstepping and sliding mode control. *Robotics and Autonomous Systems*, 152, art.number:104058. Available at: https://doi.org/10.1016/j.robot.2022.104058.

Tang, Z., Liu, H., Zhao, Z., Lu, J., Guan, H. & Chen, H. 2021. Trajectory tracking of unmanned tracked vehicle based on model-free algorithm for off-road driving conditions. In: *2021 IEEE International Conference on Unmanned Systems (ICUS)*. Beijing, China, pp.870-877, October 15-17. Available at: https://doi.org/10.1109/ICUS52573.2021.9641176.

Tao, J., Liu, H., Li, Y., Guan, H., Liu, J. & Chen, H. 2021. Design of Trajectory Tracking Controller of Unmanned Tracked Vehicles Based on Torque Control. In: *2021 IEEE International Conference on Unmanned Systems (ICUS)*. Beijing, China, pp.85-92, October 15-17. Available at: https://doi.org/10.1109/ICUS52573.2021.9641159.

Wong, J.Y. 2022. *Theory of Ground Vehicles, 5th Edition*. Hoboken, NJ, USA: John Wiley & Sons. ISBN: 978-1-119-71970-0.

Zhang, X., Zhang, X., Xue, W. & Xin, B. 2021. An overview on recent progress of extended state observers for uncertain systems: Methods, theory, and applications. *Advanced Control for Applications: Engineering and Industrial Systems*, 3(2), e89. Available at: https://doi.org/10.1002/adc2.89.

Zou, T., Angeles, J. & Hassani, F. 2018. Dynamic modeling and trajectory tracking control of unmanned tracked vehicles. *Robotics and Autonomous Systems*, 110, pp. 102–111. Available at: https://doi.org/10.1016/j.robot.2018.09.008.

Diseño sistemático de la trayectoria de un vehículo de orugas no tripulado basado en ADRC seguimiento con validación FPGA-en-el-bucle

Momir R. Stanković[a], **autor de correspondencia**,
Rafal Madonski[b], *Stojadin* M. Manojlović[a]

[a] Universidad de Defensa de Belgrado, Academia Militar, Belgrado, República de Serbia

[b] Universidad Tecnológica de Silesia, Facultad de Control Automático, Electrónica e Informática, Gliwice, República de Polonia

CAMPO: control automático, ingeniería de control, robótica móvil

TIPO DE ARTÍCULO: artículo científico original

Resumen:

Introducción/objetivo: El problema del control de seguimiento de trayectoria en un vehículo de orugas no tripulado (UTV) representa una tarea desafiante, debido a la dinámica de deslizamiento desconocida e inmensurable que inevitablemente existe durante el movimiento. Por lo tanto, la aplicación de esquemas de control industrial estándar suele ser limitada.

Métodos: En este artículo, se propone un esquema de control activo de rechazo de perturbaciones (ADRC) para los canales de control longitudinal (control de velocidad longitudinal del vehículo) y canales de control lateral (control del ángulo de trayectoria del vehículo) del UTV para manejar colectivamente todas las incertidumbres del modelado de la planta y las perturbaciones de deslizamiento actuantes.

Resultados: Se presenta un procedimiento paso a paso para aplicar el algoritmo ADRC para el caso específico de seguimiento de trayectoria de UTV. Incluye diseño sistemático, discretización, así como análisis y validación del rendimiento utilizando simulaciones FPGA-en-el-bucle (FIL).

Conclusión: El método de validación basado en FIL propuesto reduce la brecha entre el diseño de simulación pura (que puede estar demasiado idealizado) y la implementación en el vehículo real (que puede llevar mucho tiempo). Los resultados experimentales obtenidos muestran las ventajas de la estructura de control propuesta sobre los controladores PI/PID industriales.

Stanković, M. et al., Systematic design of ADRC-based unmanned tracked vehicle traj. tracking with FPGA-in-the-loop valid., pp.1700–1725

Palabras claves: vehículos de orugas no tripulados, seguimiento de trayectoria, control de rechazo activo de perturbaciones, control de velocidad, controlador PID, FPGA-en-el-bucle, validación de hardware.

Проектирование движения беспилотной гусеничной машины по заданной траектории на основе контроллера ADRC и моделирования

Момир Р. Станкович[а], **корресподент**,
Рафал Мадонски[б], *Стоядин* М. Манойлович[а]

[а] Универстет обороны в Белграде, Военная академя, г. Белград, Республика Сербия

[б] Силезский технологический университет, Факультет автоматического управления, электроники и вычислительной техники, г. Гливице, Республика Польша

РУБРИКА ГРНТИ: 50.43.00 Системы автоматического управления, регулирования и контроля

ВИД СТАТЬИ: оригинальная научная статья

Резюме:

Введение/цель: Разработка системы автономного слежения за заданной траекторией беспилотной гусеничной машины является сложной задачей из-за неизвестной и неизмеримой динамики скольжения. Поэтому применение стандартных алгоритмов промышленного управления зачастую ограничено.

Методы: В данной статье представлена схема активного управления подавлением помех (ADRC) для продольного (управление продольной скоростью транспортного средства) и бокового (управление углом наклона транспортного средства) каналов управления UTV, позволяющая в совокупности справляться со всеми неопределенностями, связанными с моделированием установки и действующими возмущениями при скольжении.

Результаты: В статье представлена пошаговая процедура применения алгоритма ADRC для конкретного случая отслеживания траектории беспилотной гусеничной машины.

Процедура включает: систематическое проектирование, дискретизацию, а также анализ производительности и валидацию с использованием моделирования FPGA-in-the-loop (FIL).

Выводы: Предлагаемый метод проверки на основе встроенного моделирования FIL сокращает разрыв между имитационным проектированием (которое может быть слишком идеализированным) и реализацией на реальном транспортном средстве (что может занять много времени). Полученные экспериментальные результаты демонстрируют преимущества предложенной системы управления по сравнению со стандартными промышленными контроллерами в различных условиях эксплуатации беспилотной гусеничной машины.

Ключевые слова: беспилотные гусеничные машины, отслеживание траектории, активное управление подавлением помех, регулирование скорости, PID-контроллер, моделирование FIL, валидация аппаратного обеспечения.

Пројектовање кретања беспосадног гусеничног возила по задатој путањи на основу ADRC регулатора и FIL симулација

Момир Р. Станковић[а], **аутор за преписку**,
Рафал Мадонски[б], *Стојадин* М. Манојловић[в]

[а] Универзитет одбране у Београду, Војна академија, Београд, Република Србија

[б] Шлески технолошки универзитет, Факултет за аутоматско управљање, електронику и рачунарство, Гливице, Република Пољска

ОБЛАСТ: аутоматско управљање, рачунарске науке, роботика
КАТЕГОРИЈА (ТИП) ЧЛАНКА: оригинални научни рад

Сажетак:

Увод/циљ: Пројектовање система аутономног праћења задате трајекторије беспосадног гусеничног возила представља сложен задатак због постојања непознате и немерљиве динамике проклизавања. Стога је примена стандардних индустријских управљачких алгоритама често ограничена.

Stanković, M. et al., Systematic design of ADRC-based unmanned tracked vehicle traj. tracking with FPGA-in-the-loop valid., pp.1700–1725

Методе: Предложена је примена регулатора на основу управљања са активним потискивањем поремећаја (ADRC), посебно пројектованих за лонгитудинални и латерални канал управљања возила. Примена наведеног алгоритма омогућила је високе перформансе управљања у условима постојања нестационарности модела објакта управљања и утицаја поремећаја проклизавања.

Резултати: Представљена је детаљна процедура примене ADRC алгоритма за праћење задате путање беспосадног гусеничног возила, која је обухватила пројектовање, дискретизацију, симулациону анализу перформанси и експерименталну верификацију на основу симулација са FPGA хардвером у петљи управљања (FIL симулације).

Закључак: Предложена методологија валидације пројектованог система управљања на основу FIL симулација омогућила је смањење пројектантског времена између чисто рачунарских симулација (које су најчешће сувише идеализоване) и експерименталних верификација на реалном систему. Добијени резултати су показали предности предложеног решења у односу на стандардне индустријске регулаторе у различитим условима употребе беспосадног гусеничног возила.

Кључне речи: беспосадно гусенично возило, праћење путање, управљање са активним потискивањем поремећаја (ADRC), управљање брзином, PID регулатор, FIL симулација, хардверска валидација.

EDITORIAL NOTE: The second author of this article, Rafal Madonski, is a current member of the Editorial Board of the Military Technical Courier. Therefore, the Editorial Team has ensured that the double blind reviewing process was even more transparent and more rigorous. The Team made additional effort to maintain the integrity of the review and to minimize any bias by having another associate editor handle the review procedure independently of the editor – author in a completely transparent process. The Editorial Team has taken special care that the referee did not recognize the author's identity, thus avoiding the conflict of interest.

Paper received on: 22.03.2024.
Manuscript corrections submitted on: 16.11.2024.
Paper accepted for publishing on: 18.11.2024.